Impact of the Specific Activity and PSMA Expression Level on ^{18}F-AlF-PSMA-11 Uptake in Prostate Cancer

Sarah Piron (sarah.piron@ugent.be)
Lab of radiopharmacy, Ghent University, Ghent, Belgium
Jeroen Verhoeven
Dept Diagnostic Sciences, Ghent University, Ghent, Belgium
Emma De Coster
Lab of radiopharmacy, Ghent University, Ghent, Belgium
Benedicte Descamps
IBiTech-MEDISIP, Dept of Electronics and Information Systems, Ghent University, Ghent, Belgium
Ken Kersemans
Dept Medical Imaging, Ghent University Hospital, Ghent, Belgium
Leen Pieters
Dept of Human Structure and Repair, Ghent University, Ghent, Belgium
Anne Vral
Dept of Human Structure and Repair, Ghent University, Ghent, Belgium
Christian Vanhove
IBiTech-MEDISIP, Dept of Electronics and Information Systems, Ghent University, Ghent, Belgium
Filip De Vos
Lab of radiopharmacy, Ghent University, Ghent, Belgium

Research Article

Keywords: PSMA, 18F-AlF-PSMA-11, specific activity, PSMA expression, prostate cancer

Posted Date: October 13th, 2021

DOI: https://doi.org/10.21203/rs.3.rs-915184/v1

Abstract

This two-part preclinical study aims to evaluate prostate specific membrane antigen (PSMA) as a valuable target for expression-based imaging applications and to determine changes in target binding in function of varying specific activities (SA) of ^{18}F-AlF-PSMA-11. For the evaluation of PSMA expression levels, male NOD/SCID mice bearing prostate cancer (PCa) xenografts of C4-2 (PSMA+++), 22Rv1 (PSMA+) and PC-3 (PSMA-) were administered ^{18}F-AlF-PSMA-11 with a medium SA (20.26 ± 3.25 MBq/μg). SUV_{mean} and SUV_{max} values were respectively 3.22 and 3.17 times higher for the high vs low PSMA expressing tumors ($p < 0.0001$). To evaluate the effect of varying SA, C4-2 and 22Rv1 xenograft bearing mice underwent additional ^{18}F-AlF-PSMA-11 imaging with a high (213.3 ± 39.3 MBq/μg) and/or low SA (1.94 ± 0.27 MBq/μg). SUV values showed a significantly increasing trend with higher SA. Significant changes were found for SUV_{mean} and SUV_{max} between the high vs low SA and medium vs low SA (both $p < 0.05$), but not between the high vs medium SA ($p = 0.055$ and 0.25, respectively). The effect of varying SA was more pronounced in low expressing tumors and PSMA expressing tissues (e.g. salivary glands and kidneys). Overall, administration of a high SA increases the detection of low expression tumors while also increasing uptake in PSMA expressing tissues, possibly leading to false positive findings. In radioligand therapy, a medium SA could reduce radiation exposure to dose-limiting organs with only limited effect on radionuclide accumulation in the tumor.

Background

Prostate specific membrane antigen (PSMA) is a type II transmembrane glycoprotein that exhibits glutamate carboxypeptidase activity in the proximal small intestines (folate hydrolase) and the brain (NAALADase)(1). Furthermore, PSMA expression can be found on several tissues including prostate tissue, renal tubules, liver, spleen, and salivary and lacrimal glands (2). In prostate cancer (PCa) cells, PSMA is expressed 100–1000 fold higher. This overexpression is positively correlated with tumor grade, pathological stage and metastatic castration-resistant prostate cancer (mCRPC), making it an attractive target for both diagnostic and therapeutic purposes (3–5).

For molecular imaging, radiopharmaceuticals are preferably produced with a high specific activity (SA) to ensure that the injected solution contains only a small amount (pico to microgram range) of the tracer substance to avoid pharmacological activity and potential toxic effects. With competitive binding of the radioligand to a target with a saturable receptor density, the chemical mass may affect receptor binding and tracer pharmacokinetics, leading to impaired imaging quality (6). This mass effect has already been described in the central nervous system, where sub-nanomolar binding affinity ranges and high specific activities are required to distinguish specific from non-specific binding (7, 8). Noguchi et al. demonstrated a positive impact of a high SA of ^{11}C-raclopride for characterization of the D_2-receptor in low density regions in the rat brain (9). For neuroendocrine tumors containing somatostatin receptors, multiple somatostatin-targeting radioligands have shown a dependency between peptide mass and radioligand uptake. Peptide mass-dependent uptake of ^{68}Ga-DOTATOC, a radiolabelled somatostatin receptor ligand,

was observed both in organs and tumor tissue (10). ^{111}In[DOTA^{0},TYR^{3}]octreotide showed an organ-dependent relationship between radioligand uptake and peptide mass, which was suggested to be a balance of the amount of peptide positively influencing receptor clustering while negatively impacting receptor saturation (11). For ^{111}In-pentreotide, a bell-shaped relationship between specific uptake in octreotide receptor-positive tissues and carrier dose was found. This introduced an additional parameter to ameliorate the target-to-background contrast. Attributing factors to this phenomenon could be receptor accessibility (blood perfusion, presence of endogenous ligand) and receptor binding properties (dissociation constant, rate of internalization and re-expression rate of the receptor) (12). These studies show that the amount of peptide administered could be optimized to increase absolute tumor uptake and tumor-to-background ratios.

The impact of the SA as a parameter for PET imaging has been investigated for several imaging targets, and it was reported to be highly pronounced for radioligands targeting PSMA. Increasing the peptide mass had predominantly an effect on uptake in PSMA expressing organs compared to tumors which seemed to be tissue-dependent (13). Soeda et al. also demonstrated a higher sensitivity of the salivary glands to increasing amounts of peptide compared to tumor tissue using ^{18}F-PSMA-1007, potentially minimizing xerostomia during PSMA radioligand therapy (RLT) (14). In this two-part preclinical study, we aim to validate PSMA as a target for expression-based imaging by determining the relationship between differences in PSMA expression levels and tumor uptake. Furthermore, changes in the specific activity/amount of peptide of ^{18}F-AlF-PSMA-11 on uptake parameters and tumor-to-organ ratios will be evaluated.

Materials And Methods

Synthesis of ^{18}F-AlF-PSMA-11. ^{18}F-AlF-PSMA-11 was synthesized on a modified SynthraFCHOL synthesis module (Synthra GmbH, Hamburg, Germany) as previously reported with some minor modifications (15). The radiochemical purity was 95.9–97.1% as determined by thin layer chromatography (Alugram RP18-W/UV254 plates (Machery Nagel, Düren, Germany)) using 3:1 v/v acetonitrile in water as mobile phase. Specific activities between 77 and 543 MBq/µg were achieved as analysed by high performance liquid chromatography (Prevail C18 reversed-phase column, 4.6×250 mm, 5 µm, Lokeren, Belgium) and a calibrated dose calibrator (Biodex medical systems, USA). To achieve differences in SA levels, varying amounts of a 0.1 µg/µL PSMA-11 (ABX) solution were added to a stock vial to obtain solutions of 1.94 ± 0.27 MBq/µg (low SA), 20.26 ± 3.25 MBq/µg (medium SA) and 213.3 ± 39.3 MBq/µg (high SA).

Preparation of tumor models. The study was approved by the Ghent University Ethical Committee on animal experiments (ECD 18/116). All animals were kept and handled according to the European guidelines (Directive 2010/63/EU). PCa cell lines C4-2 (ATCC; CRL-3314), 22Rv1 (ATCC; CRL-2505) and PC-3 (ATCC; CRL-1435) were cultured using RPMI 1640 medium supplemented with 10% FBS, 1% streptomycin/penicillin (10,000 U/mL) and 1% glutamine 200 mM, and maintained at 37°C in 5% CO_2 in humidified air. For inoculation, PCa cells were rinsed with FBS-free RPMI 1640 medium and cell

suspensions of 5×10^6 cells/100 µL were prepared. Four-to-six-week-old male NOD/SCID mice (Janvier, France) were subcutaneously injected at shoulder height with 200 µL 1:1 cell suspension:Matrigel on either side of each mouse (C4-2, n = 8; 22Rv1, n = 6; PC-3, n = 5). Tumor growth was monitored weekly for 5–6 weeks until tumors reached a diameter between 5 and 10mm.

Small animal PET/CT imaging. To evaluate the activity uptake in PCa tumors with different PSMA expression levels, all mice were injected with 9.30 ± 0.62 MBq ^{18}F-AlF-PSMA-11 with a medium SA (20.26 ± 3.25 MBq/µg). One hour post injection (p.i.), static PET/CT scans were performed for 15 minutes. To determine the impact of varying specific activities, C4-2 xenograft bearing mice underwent two additional PET/CT scans within a timeframe of two weeks. Each mouse was administered 9.29 ± 0.37 MBq ^{18}F-AlF-PSMA-11 with a high SA (196.8 ± 32.4 MBq/µg) and low SA (1.94 ± 0.274 MBq/µg). 22Rv1 xenograft bearing mice underwent one additional PET/CT scan within one week. Each mouse was administered 9.47 ± 0.24 MBq ^{18}F-AlF-PSMA-11 with a high SA of 246.3 ± 33.1 MBq/µg.

The images were acquired in list mode using a small animal PET scanner (β-cube, Molecubes, Ghent, Belgium) with a spatial resolution of 0.85 mm and an axial field-of-view of 13 cm. All PET scans were reconstructed into a 192×192×384 matrix by an ordered subsets maximization expectation (OSEM) algorithm using 30 iterations and a voxel size of 400 µm.

Immunohistochemical evaluation. After the last scan, two mice/cell line xenograft were sacrificed and tumors were collected for immunohistochemical (IHC) evaluation. Sections were stained using Haematoxylin/Eosin, incubated with a primary PSMA antibody (1:400, 2h, ab133579, Abcam) and counterstained using Haematoxylin (Mayer). Sections were digitally scanned with a virtual scanning microscope (Olympus BX51, Olympus Belgium SA/NV, Berchem, Belgium) at high resolution (20× magnification).

Western blot analysis. The remaining tumors were harvested for western blot (WB) analysis to quantify the PSMA expression levels of the tumor tissues. After thorough rinsing of the tumors, tissue lysates were prepared using RIPA sample buffer. Protein concentrations were determined using the Pierce BCA Protein assay (ThermoFisher Scientific). Samples containing 50 µg of total protein were loaded on 8.5% sodium dodecyl sulphate-polyacrylamide gel electrophoresis (SDS-PAGE) gels. After the transfer, the nitrocellulose membranes were blocked using Odyssey Blocking Buffer (Li-cor Biosciences, Bad Homburg, Germany). Membranes were incubated overnight using a monoclonal PSMA Rabbit anti-Human primary antibody (1:2000, MA533086, Invitrogen, Fischer Scientific, Belgium) and polyclonal Rabbit anti-Human beta actin primary antibody (1:1000, PA1-183, Invitrogen, Fischer Scientific, Belgium), followed by 1h incubation with IRDye® 800CW Goat anti-Rabbit IgG secondary antibody (1:15000, Li-cor Biosciences, Bad Homburg, Germany). The relative densities of both PSMA and β-actin bands were determined using ImageJ (16).

Data analysis. Co-registration and analysis of the PET/CT images was performed using PMOD (PMOD Technologies®, Zürich, Switzerland). Images were visually analysed using the PROMISE criteria. This

standardizes image interpretation based on activity uptake in reference tissues (blood, liver and salivary gland) and subdivides suspicious lesions into no, low, intermediate or high PSMA expression (17). Volumes of interest (VOIs) were drawn manually for delineating the tumor, kidneys, bladder, salivary and lacrimal glands, heart (blood), liver, spleen, muscle and bone. Tissue uptake in each VOI was corrected for residual activity in the syringe and radioactive decay,wq and expressed as SUV_{mean} and SUV_{max} according to Formula 1. Furthermore, tumor-to-organ ratios of tissues with a high likelihood for metastases including tumor-to-liver (TLR), tumor-to-muscle (TMR) and tumor-to-bone ratio (TBoR) were determined.

$$SUV = \frac{(Maximum)\ ActivityVOI\left(\frac{MBq}{mL}\right)}{Injecteddose\,(MBq)} \times BodyWeight(g) \quad \textit{Formula 1}$$

Statistical analysis. All uptake parameters (SUV_{mean}, SUV_{max}, TLR, TMR and TBoR) were reported as mean ± SD. The statistical analysis was performed in R (18) using the Mann-Whitney U test for comparison of uptake between different PSMA expressing xenografts and the Kruskal Wallis test for comparing radioligand uptake of varying SA, followed by post-hoc pairwise comparison using the Wilcoxon-signed rank test with holm correction for multiple testing. The significance level was set on $p \leq 0.05$.

Results

Semi-quantitative analysis of PSMA expression levels in prostate cancer cell lines.

The PSMA expression levels were determined by both western blot and immunohistochemical assessment (Fig. 1). WB analysis detected the highest presence of PSMA expression in C4-2 tissue, while only moderate to low expression levels could be observed for 22Rv1. Semi-quantification of blots revealed a β-actin normalized density for PSMA expression of 16.36 ± 3.05 for C4-2 and 0.94 ± 0.21 for 22Rv1 tumors. PC-3 tumors did not show PSMA expression. Similar results were demonstrated by IHC staining, where all C4-2 cells were clearly positively stained for PSMA, while 22Rv1 showed weaker and more heterogeneous staining of the tumor tissue.

Relationship between PSMA expression levels and ^{18}F-AlF-PSMA-11 tumor uptake.

Comparative images of ^{18}F-AlF-PSMA-11 uptake (medium SA) in different PSMA expressing tumors are presented in Fig. 2. Tumor uptake was positively correlated with higher expression levels. According to the PROMISE criteria, PC-3 tumors were PSMA negative (score 0) as tumor uptake was comparable with activity in the blood (heart). 22Rv1 tumors were visually detectable and the tumor activity was higher than the liver but lower than salivary glands, which corresponds to intermediate PSMA expression (score 2). C4-2 tumors showed good image contrast with tumor uptake above activity in the salivary glands (score 3).

Quantitative VOI analysis demonstrated significant differences for SUV_{mean} and SUV_{max} as well as tumor-to-organ ratios including tumor-to-liver, tumor-to-blood and tumor-to-muscle in function of PSMA expression levels (Table 1). When comparing C4-2 (high PSMA expression) to 22Rv1 (low PSMA expression), SUV_{mean} and SUV_{max} values were approximately 3.22 and 3.17 times higher, respectively ($p < 0.0001$). Similar ratios of 2.77, 2.23 and 2.96 were found for tumor-to-liver, tumor-to-blood and tumor-to-muscle, respectively ($p < 0.0001$). SUV values were significantly lower for PC-3 tumors compared to both C4-2 ($p < 0.01$) and 22Rv1 tumors ($p < 0.001$).

*Table 1: SUV values and tumor-to-organ ratios (liver, blood and bone) for different PCa tumor cell lines with varying PSMA expression levels: PC-3 (no PSMA expression), 22Rv1 (low PSMA expression) and C4-2 (high PSMA expression). P-values were calculated using the Wilcoxon signed-rank test with Holm correction with C4-2 as a reference, the significance level was set at p = 0.05, ** = p<0.01, **** = p< 0.0001. [a]Expression levels were determined by semi-quantitative western blot analysis and are expressedβ-actin normalized density. [b]Activity in blood was determined by delineation of the heart.*

Cell line	Expression level[a]	SUVmean	SUVmax	Tumor-to-liver ratio	Tumor-to-blood ratio[b]	Tumor-to-muscle ratio
PC-3	0	0.09 ± 0.02**	0.22 ± 0.05**	1.38 ± 0.33**	1.41 ± 0.07**	2.26 ± 0.48**
22Rv1	0.94 ± 0.21	0.46 ± 0.11****	1.03 ± 0.23****	6.26 ± 1.41****	6.93 ± 1.49****	6.64 ± 3.81****
C4-2	16.36 ± 3.05	1.48 ± 0.47	3.27 ± 1.07	17.32 ± 3.55	15.47 ± 2.32	19.64 ± 5.37

Impact of the specific activity on tumor uptake.

To evaluate the impact of the SA on tumor uptake, all C4-2 xenograft bearing mice underwent three PET/CT scans with different SA levels (high SA = 196.8 ± 32.4 MBq/µg, medium SA = 19.10 ± 1.69 MBq/µg and low SA = 1.94 ± 0.27 MBq/µg). Images show high uptake in C4-2 tumors after injection of a high SA activity dose, which decreased with lower SA (Fig. 3). Kidney uptake decreased as well with lower SA while activity in de bladder increased. PSMA expressing tissues such as salivary glands, lacrimal glands and spleen were clearly visible on high SA PET images but were barely visible on medium SA images and not detectable on low SA images.

When comparing intra-individual tumor uptake of the high, medium and low SA, SUV_{mean} (2.14 ± 0.54, 1.48 ± 0.47 and 0.58 ± 0.10, respectively) and SUV_{max} (4.44 ± 1.25, 3.27 ± 1.07 and 1.15 ± 0.19, respectively) showed a significantly decreasing trend (both $p < 0.001$). Post-hoc pairwise comparison revealed statistically significant changes between the high and low SA ($p < 0.05$) as well as between the medium and high SA ($p < 0.05$), but not between the high and medium SA ($p = 0.055$ and 0.25, respectively) (Fig. 4a). Additionally, 22Rv1 xenograft bearing mice (n = 3) received an additional PET/CT

scan with high SA (246.3 ± 33.1 MBq/μg). Comparison of SUV_{mean} and SUV_{max} values demonstrated a statistically significant difference between the high and medium SA (both p = 0.031).

Tumor-to-organ ratios were determined for tissues with a high likelihood for metastases including liver (TLR), muscle (lymph nodes) (TMR) and bone (TBoR). In C4-2 xenografts, tumor-to-organ ratios remained constant between the high and medium SA for TLR (15.71 ± 1.99 vs 17.32 ± 3.55, p = 0.46), TMR (20.69 ± 3.82 vs 19.64 ± 5.37, p = 0.74) and TBoR (3.77 ± 0.78 vs 3.33 ± 1.03, p = 0.31) while a statistically significant difference could be observed for high vs low SA and medium vs low SA (Fig. 4b). A similar trend between the high and medium SA was found for 22Rv1 xenografts, however, the tumor-to-liver ratio remained constant. On the other hand, SUV_{mean} values of PSMA expressing tissues such as salivary and lacrimal glands, spleen, and kidneys significantly decreased between the high and medium SA ($p < 0.01$) (Fig. 5). Tumor-to-salivary gland ratios increased from 2.30 ± 0.37 for the high SA to 5.35 ± 0.59 for the medium SA. While kidney uptake significantly decreased, uptake in the bladder rose for the medium and low SA.

Discussion

Although the diagnostic applications of PSMA as a target for imaging have been the subject of many clinical trials, preclinical studies are essential for a comprehensive investigation of several important aspects of PSMA PET imaging. In this paper, ^{18}F-AlF-PSMA-11 was used for imaging experiments to further understand PSMA PET imaging. First, PSMA was validated as a valuable target for expression-based applications by determining the relationship between PSMA expression levels and ^{18}F-AlF-PSMA-11 tumor uptake. This was examined using three human PCa cell lines with high (C4-2), low (22Rv1) and no detectable (PC-3) PSMA expression. Second, changes in target binding of PSMA positive tumors and tissues using varying amounts of cold PSMA-11 peptide were evaluated.

The relationship between target expression levels and ^{18}F-AlF-PSMA-11 uptake was determined by PET/CT imaging of mice bearing PCa tumors with varying PSMA expression levels. The use of a medium SA for the expression level experiments was selected based on several practical considerations. A larger group of mice could be imaged on the same day, while the use of the high SA would significantly limit the size of the study population. Also, using the high SA would introduce a larger variation in the SA between animals, as the amount of PSMA-11 precursor is so small, that minor differences would lead to large differences is SA. Semi-quantitative western blot analysis showed that PSMA expression levels of C4-2 tumors were approximately 16 times higher compared to 22Rv1 tumors, while SUV values were only 3 times higher. A positive association between PSMA expression and SUV values could be found, although there was no significant linear correlation ($p > 0.05$). Although 22Rv1 tumors had only low PSMA expression levels on western blot, activity uptake was above the liver, scoring positively (score 2) according to the PROMISE criteria. This suggests the ability of ^{18}F-AlF-PSMA-11 to detect PCa lesions, even with low PSMA receptor abundancy. Increasing the SA of ^{18}F-AlF-PSMA-11 increased absolute SUV_{mean} and SUV_{max} values (Fig. 4), but due to higher salivary gland uptake, the PROMISE score did not

increase. However, TMR and TBoR did increase significantly, which could be beneficial for the detection of lymph nodes and bone metastases with low PSMA expression levels, although this should be confirmed in a murine model of bone metastases. Lückerath et al. determined the *in vivo* correlation between ^{68}Ga-PSMA-11 PET/CT and PSMA expression using four murine PCa cell lines. ^{68}Ga-PSMA-11 PET was able to detect changes in PSMA expression at low levels, but this sensitivity was lost at higher PSMA levels, which is in agreement with the reported non-linear correlation (19).

PSMA expression was shown to be an important prognosticator for overall survival of metastatic castrate resistant prostate cancer (mCRPC) patients under ^{177}Lu-PSMA treatment. The presence of low average-PSMA expressing tumors was found to be a negative prognostic factor in these patients (20). The threshold for determining the PSMA expression level was based on the criterium set by Hofman et al. who defined high PSMA expression as any metastatic lesion with a SUV_{max} of 1.5 times the liver SUV. Here, ^{177}Lu-PSMA therapy resulted in 50% decline in PSA for 17/30 mCRPC patients presenting with high PSMA expression metastases (21). The liver seems to be a solid choice as reference organ as our results show that changes in the SA did not significantly alter tumor-to-liver ratios (between the high and medium SA). Additional research should determine to which extent PSMA expression levels could be used as an exclusion criterium for ^{177}Lu-PSMA therapy. In our study, the difference between the medium and high SA was more pronounced in low expression 22Rv1 tumors. SUV values, TMR and TBoR increased significantly when administering the high SA. This can be attributed to the lower amount of receptors available to bind radiolabelled PSMA molecules and more rapid saturation in the presence of a larger peptide mass.

Overall, the highest mean absolute SUV_{mean} and SUV_{max} values were obtained after administration of ^{18}F-AlF-PSMA-11 with high SA, but the difference between the medium and high SA was not statistically significant, both for SUV values as for tumor-to-organ ratios (TLR, TMR and TBoR). There was however a substantial decrease of activity uptake in PSMA expressing tissues (salivary and lacrimal glands, spleen and kidneys) between the high and medium SA. The use of medium SA ^{18}F-AlF-PSMA-11 could therefore reduce activity uptake in PSMA positive healthy tissues while maintaining image contrast of tumor metastases compared to the surrounding tissue. This would be beneficial for both diagnostic purposes and radioligand therapy. Prostate cancer lesions could be more reliably detected due to the constant tumor-to-organ ratio while less non-specific uptake could facilitate scan interpretation by limiting the potential pitfalls of PSMA PET caused by aspecific physiological uptake (22). In radioligand therapy, healthy tissue would be less exposed to the radiation while absolute tumor uptake would remain approximately constant.

During PSMA radioligand therapy, radiation exposure caused by activity uptake in PSMA-expressing non-tumor tissues can cause dose-limiting toxic side effects. Radioligand uptake in the salivary glands causes xerostomia and can be a reason for treatment discontinuation (23, 24). Lowering the SA for RLT ligands could be a useful tool for reducing radiation exposure and should be further investigated as an alternative for botulinum toxin injections (25) or sialendoscopy and dilatation combination with saline

irrigation and steroid injections (26). A preclinical study by Fendler et al. also showed that administration of ^{177}Lu-PSMA-617 with a molar activity of 62 MBq/nmol achieved the highest tumor-to-salivary gland ratio compared to lower molar activities (31 and 15 MBq/nmol) (27). When correcting for the administered dose of 60 MBq, the highest molar activity corresponds to 0.97 nmol PSMA-617, which is in the same range as our medium SA group (0.49 nmol PSMA-11) that also showed the highest tumor-to-salivary gland ratio. However, it was reported that the low to moderate PSMA staining on IHC staining does not correlate with the high PSMA radioligand accumulation. It was hypothesized that tracer accumulation in the salivary glands is therefore a combination of both specific and non-specific uptake (28). The latter mechanism is not yet elucidated and our results show a large impact of a higher amount of peptide on activity uptake in salivary glands, suggesting that this as a promising direction for further research. Another organ-at-risk are the kidneys. Renal clearance can lead to accumulation of radiolabelled peptides in the tubular cells where it irradiates the kidneys, potentially leading to renal dysfunction, particularly in patients with a known history of nephropathy. Although no major nephrotoxicity was reported for ^{177}Lu-PSMA (29), chronic kidney disease was reported in two patients for ^{225}Ac-PSMA therapy. Limiting kidney exposure to ^{255}Ac-PSMA may decrease toxicity and maintain its therapeutic potential (30). Additionally, a high tumor load in patients can also lead to reduced activity uptake in dose-limiting organs (31). ^{18}F-AlF-PSMA-11 might therefore be applied as a diagnostic tool for individual optimization of RLT protocols considering PET-based tumor load and radioligand SA.

These results show the importance of the amount of carrier on tumor targeting strategies. The optimal amount should be low to avoid competitive binding of unlabelled molecules at the target site but not too low as the tracer molecules could be trapped in non-specific binding places. For diagnostic purposed, using a high SA will increase the detection of low expression tumors while also increasing specific uptake in PSMA expressing tissues, possibly leading to false positive findings. For radioligand therapy, further research should focus on finding a balance between administration of a high SA for high absolute uptake in the tumor tissue while minimizing activity uptake in healthy organs in order to reduce dose-limiting toxicity. Also, although the considerations mentioned before are valid for high PSMA expressing PCa lesions, decreasing the SA to limit non-specific uptake could also affect the detectability of low PSMA expressing lesions, which could lead to an underestimation of the tumor burden.

A major limitation of this study is the translation from mouse to human. Although the differences in the administered SA in mice gave well defined results, the activity dose and amount of peptide that is administered compared to total body weight for PET/CT is different for mice and humans, which makes translation into clinical applications more challenging. However, as the specific activity of a PSMA PET tracer decreases over time, it would be beneficial to evaluate the effect on both tumor uptake and non-target uptake in humans. In a retrospective analysis of patients who underwent ^{18}F-rhPSMA-7.3 PET/CT, only minor effects on biodistribution were found for a 10-fold decrease of SA, except for the salivary glands and spleen, which showed significantly lower uptake for the lower specific activity (32). These results encourage a prospective clinical trial comparing a high to medium SA. Due to the intra-individual comparison of SA levels, most mice were imaged multiple times and tumor sizes differed slightly

between scans. However, the tumor size was many times higher than the PET resolution and mice were randomized for SA sequence, therefore minimizing this limitation as much as possible.

Conclusion

This paper evaluated ^{18}F-AlF-PSMA-11 PET for expression-based imaging of prostate cancer and the effect of the amount of carrier administered on tumor uptake and tumor-to-organ ratios. A positive association was found between PSMA expression and tumor uptake. The highest absolute tumor uptake was obtained by the high SA. And although activity uptake in PSMA expressing organs decreased significantly with lower SA, there was no statistically significant difference in tumor SUV between the high and medium SA. These results suggest that administration of a high SA increases the detection of low expression tumors while also increasing specific uptake in PSMA expressing tissues, possibly leading to false positive findings. In radioligand therapy, a medium SA could reduce radiation exposure to dose-limiting organs with only limited effect on radionuclide accumulation in the tumor. Overall, it is of utmost importance to validate the association between both PSMA expression and specific activity relative to radioligand activity uptake.

Abbreviations

CT = computed tomography; IHC = immunohistochemistry; mCRPC = metastatic castrate resistant prostate cancer; NAALADase = N-acetylated-α-linked-acidic dipeptidase; OSEM = ordered subsets maximization expectations; PCa = prostate cancer; PET = positron emission tomography; PSMA = prostate specific membrane antigen; RLT = radioligand therapy; SA = specific activity; SDS-PAGE = sodium dodecyl sulphate-polyacrylamide gel electrophoresis; SUV = standardized uptake value; TBoR = tumor-to-bone ratio; TLR = tumor-to-liver ratio; TMR = tumor-to-muscle ratio; VOI = volume of interest; WB = western blot

Declarations

Ethics approval and consent to participate: Thestudy was approved by the Ghent University Ethical Committee on animal experiments (ECD 18/116). All animals were kept and handled according to the European guidelines (Directive 2010/63/EU). The manuscript complies with the ARRIVE guidelines.

Availability of data and materials: The datasets and images used and/or analysed during the current study are available from the corresponding author on reasonable request.

Competing interests: The authors declare that they have no competing interests

Funding: The study was supported by the Flemish foundation FWO TBM (T001517).

Authors' contributions:SP, JV, KK and FDV contributed to the study concept and study design, data was collected by SP, JV, FDC, BD, KK, LP and OV.The manuscript was writing by SP. All authors revised and

approved the final manuscript.

Acknowledgements: The authors would like to thank the cyclotron team of the department nuclear medicine of Ghent University Hospital for the production of the radiotracer and the outstanding cooperation.

References

1. Barinka C, Rojas C, Slusher B, Pomper M. Glutamate Carboxypeptidase II in Diagnosis and Treatment of Neurologic Disorders and Prostate Cancer. Curr Med Chem [Internet]. 2012 Feb 1 [cited 2019 Aug 20];19(6):856–70. Available from: http://www.eurekaselect.com/openurl/content.php?genre=article&issn=0929-8673&volume=19&issue=6&spage=856
2. Silver DA, Pellicer I, Fair WR, Heston WDW, Cordon-Cardo2 C. Prostate-specific Membrane Antigen Expression in Normal and Malignant Human Tissues'. Clin Cancer Res [Internet]. 1997 [cited 2018 Apr 23];3(81):81–5. Available from: http://clincancerres.aacrjournals.org/content/clincanres/3/1/81.full.pdf
3. Bostwick DG, Pacelli A, Blute M, Roche P, Murphy GP. Prostate specific membrane antigen expression in prostatic intraepithelial neoplasia and adenocarcinoma: A study of 184 cases. Cancer [Internet]. 1998 Jun 1 [cited 2019 Jul 4];82(11):2256–61. Available from: http://www.ncbi.nlm.nih.gov/pubmed/9610707
4. Ross JS, Sheehan CE, Fisher HAG, Kaufman RP, Kaur P, Gray K, et al. Correlation of Primary Tumor Prostate-Specific Membrane Antigen Expression with Disease Recurrence in Prostate Cancer. Clin Cancer Res [Internet]. 2003 [cited 2018 Apr 23];9(17):6357–62. Available from: http://clincancerres.aacrjournals.org/content/clincanres/9/17/6357.full.pdf
5. Bravaccini S, Puccetti M, Bocchini M, Ravaioli S, Celli M, Scarpi E, et al. PSMA expression: A potential ally for the pathologist in prostate cancer diagnosis. Sci Rep [Internet]. 2018 [cited 2021 Jul 6];8(1):4254. Available from: www.nature.com/scientificreports/
6. Kung MP, Kung HF. Mass effect of injected dose in small rodent imaging by SPECT and PET. Vol. 32, Nuclear Medicine and Biology. Elsevier Inc.; 2005. p. 673–8.
7. Nebel N, Maschauer S, Kuwert T, Hocke C, Prante O. In vitro and in vivo characterization of selected fluorine-18 labeled radioligands for PET imaging of the dopamine D3 receptor. Molecules [Internet]. 2016 Sep 1 [cited 2021 Jun 15];21(9). Available from: /pmc/articles/PMC6272905/
8. Javed MR, Chen S, Lei J, Collins J, Sergeev M, Kim HK, et al. High yield and high specific activity synthesis of [18F]fallypride in a batch microfluidic reactor for micro-PET imaging. Chem Commun [Internet]. 2014 Jan 2 [cited 2021 Jun 15];50(10):1192–4. Available from: /pmc/articles/PMC4479166/
9. Noguchi J, Zhang MR, Yanamoto K, Nakao R, Suzuki K. In vitro binding of [11C]raclopride with ultrahigh specific activity in rat brain determined by homogenate assay and autoradiography. Nucl Med Biol. 2008 Jan 1;35(1):19–27.

10. Velikyan I, Sundin A, Eriksson B, Lundqvist H, Sörensen J, Bergström M, et al. In vivo binding of [68Ga]-DOTATOC to somatostatin receptors in neuroendocrine tumors - impact of peptide mass. Nucl Med Biol. 2010 Apr 1;37(3):265–75.
11. De Jong M, Breeman WAP, Bernard BF, Van Gameren A, De Bruin E, Bakker WH, et al. Tumor uptake of the radiolabelled somatostatin analogue [DOTA0,TYR3]octreotide is dependent on the peptide amount. Eur J Nucl Med [Internet]. 1999 [cited 2021 Jun 15];26(7):693–8. Available from: https://pubmed.ncbi.nlm.nih.gov/10398816/
12. Breeman WAP, Kwekkeboom DJ, Kooij PPM, Bakker WH, Hofland LJ, Visser TJ, et al. Effect of Dose and Specific Activity on Tissue Distribution of Indium-111-Pentetreotide in Rats. J Nucl Med [Internet]. 1995 Apr 1;36(4):623 LP – 627. Available from: http://jnm.snmjournals.org/content/36/4/623.abstract
13. Wurzer A, Pollmann J, Schmidt A, Reich D, Wester HJ, Notni J. Molar Activity of Ga-68 Labeled PSMA Inhibitor Conjugates Determines PET Imaging Results. Mol Pharm [Internet]. 2018 Sep 4 [cited 2021 Jul 2];15(9):4296–302. Available from: https://pubmed.ncbi.nlm.nih.gov/30011372/
14. Soeda F, Watabe T, Naka S, Liu Y, Horitsugi G, Neels OC, et al. Impact of 18F-PSMA-1007 uptake in prostate cancer using different peptide concentrations: Preclinical PET/CT study on mice. J Nucl Med [Internet]. 2019 Nov 1 [cited 2020 Jul 30];60(11):1594–9. Available from: https://pubmed.ncbi.nlm.nih.gov/30902876/
15. Kersemans K, De Man K, Courtyn J, Van Royen T, Piron S, Moerman L, et al. Automated radiosynthesis of Al[18 F]PSMA-11 for large scale routine use. Appl Radiat Isot [Internet]. 2018 May;135:19–27. Available from: https://linkinghub.elsevier.com/retrieve/pii/S096980431731134X
16. Schneider CA, Rasband WS, Eliceiri KW. NIH Image to ImageJ: 25 years of image analysis [Internet]. Vol. 9, Nature Methods. Nature Publishing Group; 2012 [cited 2021 Jul 9]. p. 671–5. Available from: https://www.nature.com/articles/nmeth.2089
17. Eiber M, Herrmann K, Calais J, Hadaschik B, Giesel FL, Hartenbach M, et al. Prostate cancer molecular imaging standardized evaluation (PROMISE): Proposed miTNM classification for the interpretation of PSMA-ligand PET/CT. J Nucl Med. 2018 Mar 1;59(3):469–78.
18. R Core Team. R: A language and environment for statistical computing. R Foundation for Statistical Computing [Internet]. 2019 [cited 2019 Jun 5]. Available from: https://www.r-project.org/
19. Lückerath K, Stuparu AD, Wei L, Kim W, Radu CG, Mona CE, et al. Detection Threshold and Reproducibility of 68Ga-PSMA11 PET/CT in a Mouse Model of Prostate Cancer. J Nucl Med [Internet]. 2018 Sep 1 [cited 2021 Jul 8];59(9):1392–7. Available from: /pmc/articles/PMC6910618/
20. Seifert R, Seitzer K, Herrmann K, Kessel K, Schäfers M, Kleesiek J, et al. Analysis of PSMA expression and outcome in patients with advanced Prostate Cancer receiving 177Lu-PSMA-617 Radioligand Therapy. Theranostics [Internet]. 2020 [cited 2021 Jul 26];10(17):7812–20. Available from: /pmc/articles/PMC7359095/
21. Hofman MS, Violet J, Hicks RJ, Ferdinandus J, Ping Thang S, Akhurst T, et al. [177 Lu]-PSMA-617 radioligand therapy in patients with metastatic castration-resistant prostate cancer (LuPSMA

trial): a single-centre, single-arm, phase 2 study. Lancet Oncol. 2018 Jun 1;19(6):825–33.

22. Mei R, Farolfi A, Castellucci P, Nanni C, Zanoni L, Fanti S. PET/CT variants and pitfalls in prostate cancer: What you might see on PET and should never forget. Seminars in Nuclear Medicine. W.B. Saunders; 2021.
23. Kratochwil C, Bruchertseifer F, Rathke H, Hohenfellner M, Giesel FL, Haberkorn U, et al. Targeted α-therapy of metastatic castration-resistant prostate cancer with 225 Ac-PSMA-617: Swimmer-Plot Analysis Suggests efficacy regarding duration of tumor control. J Nucl Med [Internet]. 2018 May 1 [cited 2021 Jul 16];59(5):795–802. Available from: https://jnm.snmjournals.org/content/59/5/795
24. Langbein T, Chaussé G, Baum RP. Salivary gland toxicity of PSMA radioligand therapy: Relevance and preventive strategies. J Nucl Med. 2018;59(8):1172–3.
25. Baum RP, Langbein T, Singh A, Shahinfar M, Schuchardt C, Volk GF, et al. Injection of Botulinum Toxin for Preventing Salivary Gland Toxicity after PSMA Radioligand Therapy: an Empirical Proof of a Promising Concept. Nucl Med Mol Imaging (2010) [Internet]. 2018 Feb 1 [cited 2021 Jul 16];52(1):80–1. Available from: /pmc/articles/PMC5777965/
26. Rathke H, Kratochwil C, Hohenberger R, Giesel FL, Bruchertseifer F, Flechsig P, et al. Initial clinical experience performing sialendoscopy for salivary gland protection in patients undergoing 225Ac-PSMA-617 RLT. Eur J Nucl Med Mol Imaging [Internet]. 2019 Jan 1 [cited 2021 Jul 16];46(1):139–47. Available from: https://pubmed.ncbi.nlm.nih.gov/30151743/
27. Fendler WP, Stuparu AD, Evans-Axelsson S, Lückerath K, Wei L, Kim W, et al. Establishing 177 Lu-PSMA-617 Radioligand Therapy in a Syngeneic Model of Murine Prostate Cancer. J Nucl Med [Internet]. 2017 Nov [cited 2021 Jul 16];58(11):1786–92. Available from: http://jnm.snmjournals.org/lookup/doi/10.2967/jnumed.117.193359
28. Rupp NJ, Umbricht CA, Pizzuto DA, Lenggenhager D, Töpfer A, Müller J, et al. First clinicopathologic evidence of a non-PSMA-related uptake mechanism for 68Ga-PSMA-11 in salivary glands. J Nucl Med [Internet]. 2019 [cited 2021 Aug 9];60(9):1270–6. Available from: https://pubmed.ncbi.nlm.nih.gov/30737300/
29. Gallyamov M, Meyrick D, Barley J, Lenzo N. Renal outcomes of radioligand therapy: Experience of 177lutetium-prostate-specific membrane antigen ligand therapy in metastatic castrate-resistant prostate cancer. Clin Kidney J [Internet]. 2021 Dec 28 [cited 2021 Jul 27];13(6):1049–55. Available from: https://academic.oup.com/ckj/article/13/6/1049/5549858
30. A. Scheinberg D, R. McDevitt M. Actinium-225 in Targeted Alpha-Particle Therapeutic Applications. Curr Radiopharm [Internet]. 2012 Oct 30 [cited 2021 Jul 28];4(4):306–20. Available from: /pmc/articles/PMC5565267/
31. Gaertner FC, Halabi K, Ahmadzadehfar H, Kürpig S, Eppard E, Kotsikopoulos C, et al. Uptake of PSMA-ligands in normal tissues is dependent on tumor load in patients with prostate cancer. Oncotarget [Internet]. 2017 [cited 2021 Jul 26];8(33):55094–103. Available from: /pmc/articles/PMC5589644/
32. Langbein T, Wurzer A, Gafita A, Robertson A, Wang H, Arcay A, et al. The Influence of Specific Activity on the Biodistribution of 18F-rhPSMA-7.3: A Retrospective Analysis of Clinical Positron Emission

Tomography Data. J Nucl Med [Internet]. 2021 Aug 12 [cited 2021 Aug 30];jnumed.121.262471. Available from: https://jnm.snmjournals.org/content/early/2021/08/12/jnumed.121.262471

Figures

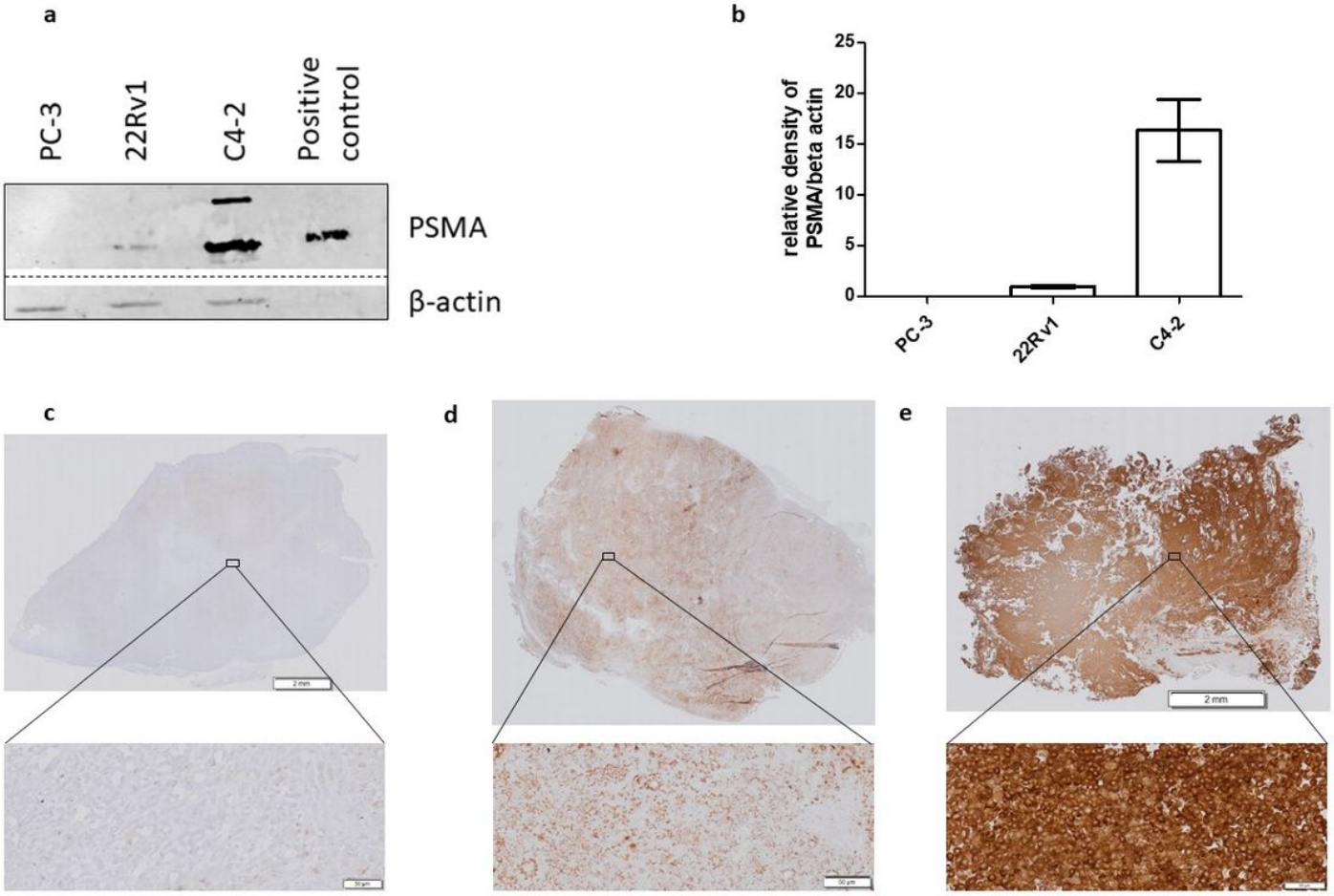

Figure 1

Analysis of PSMA expression levels. WBof PCa tumor tissues and a positive control, all samples were run on the same blot. The non-relevant bands were cropped from the image, the full-length blot is presented in Supplementary Figure 1 (a). Semi-quantification of WB, the relative density of PSMA was normalized using β-actin as loading control. Quantification was only performed using bands from the same blot (b). Data for PC-3, 22Rv1 and C4-2 (n=5)is presented as mean ± SD. IHC of PSMA expression of PC-3 (c), 22Rv1 (d) and C4-2 (e) tumor tissue.

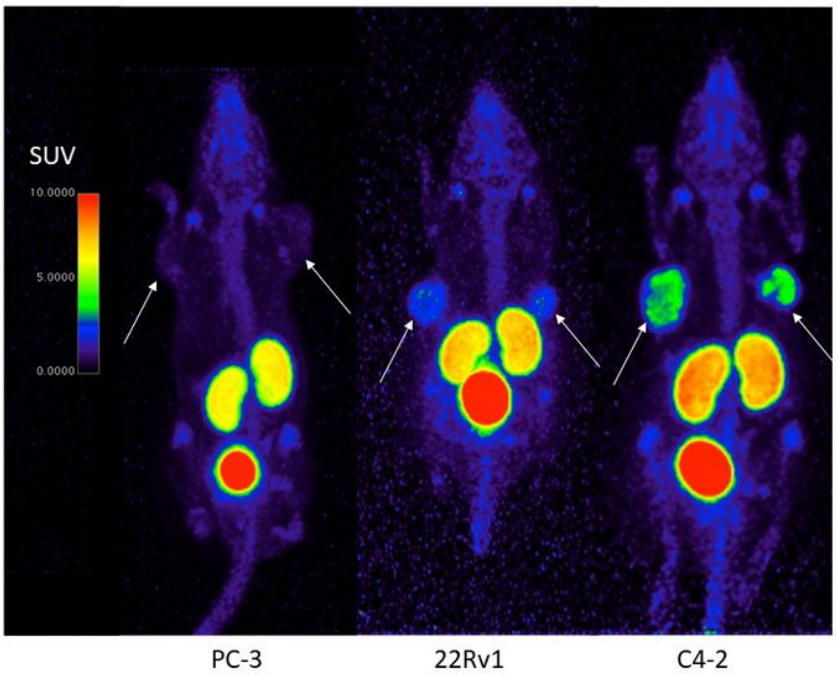

Figure 2

Representative PET images of PC-3 (left), 22Rv1 (middle) and C4-2 (right) xenografts 60 min p.i. of18F-AlF-PSMA-11 with medium SA. Arrows indicate tumors. There was no activity uptake detectable in PC-3 tumors, C4-2 and 22Rv1 tumors were visible, although the latter showed less tumor contrast.

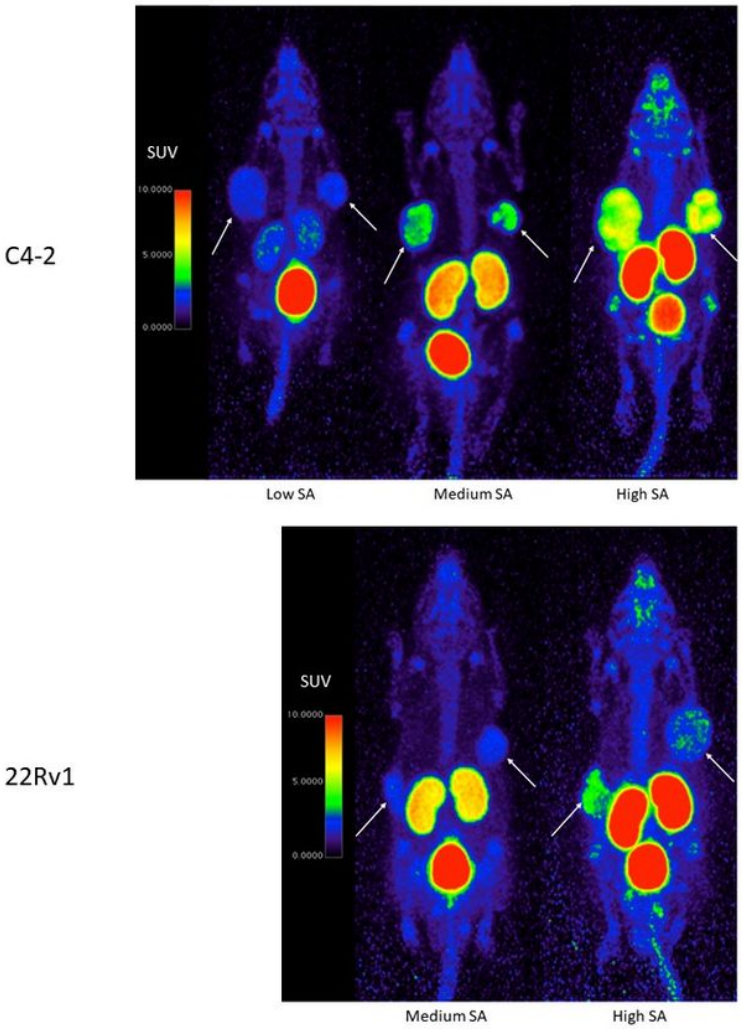

Figure 3

Representative PET images after18F-AlF-PSMA-11 injectionof C4-2 (top)and 22Rv1 (bottom) xenograftsof low (only C4-2), medium and high SA images in the same animal. Arrows indicate tumors. Increasing SA resulted in higher activity uptake in tumors as well as the kidneys, while activity in the bladder decreased.

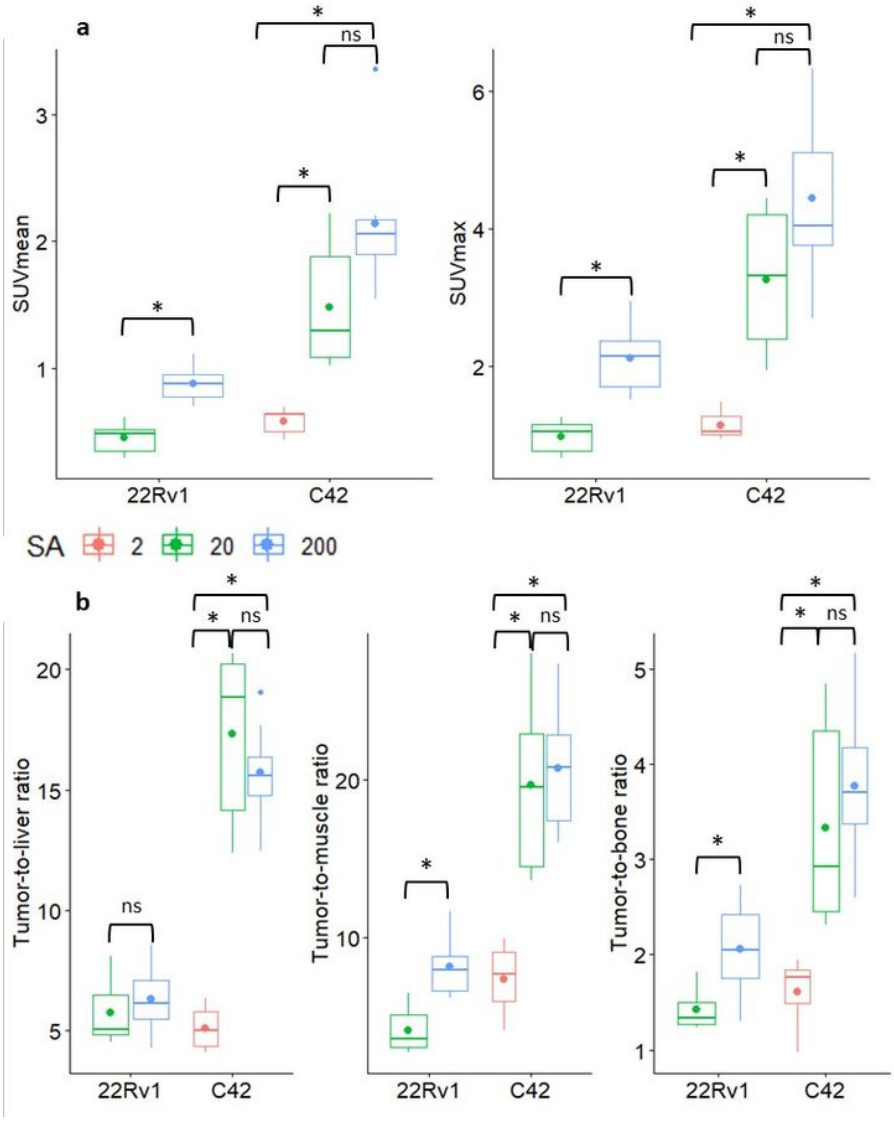

Figure 4

SUVmean and SUVmax (a) andtumor-to-liver, tumor-to-muscle and tumor-to-bone ratio(b) of 22Rv1 and C4-2 tumors after imaging with either the low SA(0.94 ± 0.27 MBq/µg, only C4-2), medium SA (20.26 ± 3.25MBq/µg) or high SA (213.3 ± 39.3 MBq/µg)18F-AlF-PSMA-11 60 minutes p.i.. The mean values were added as dots to the boxplot. The significance level was set at p=0.05.Ns = not significant, * = p<0.05.

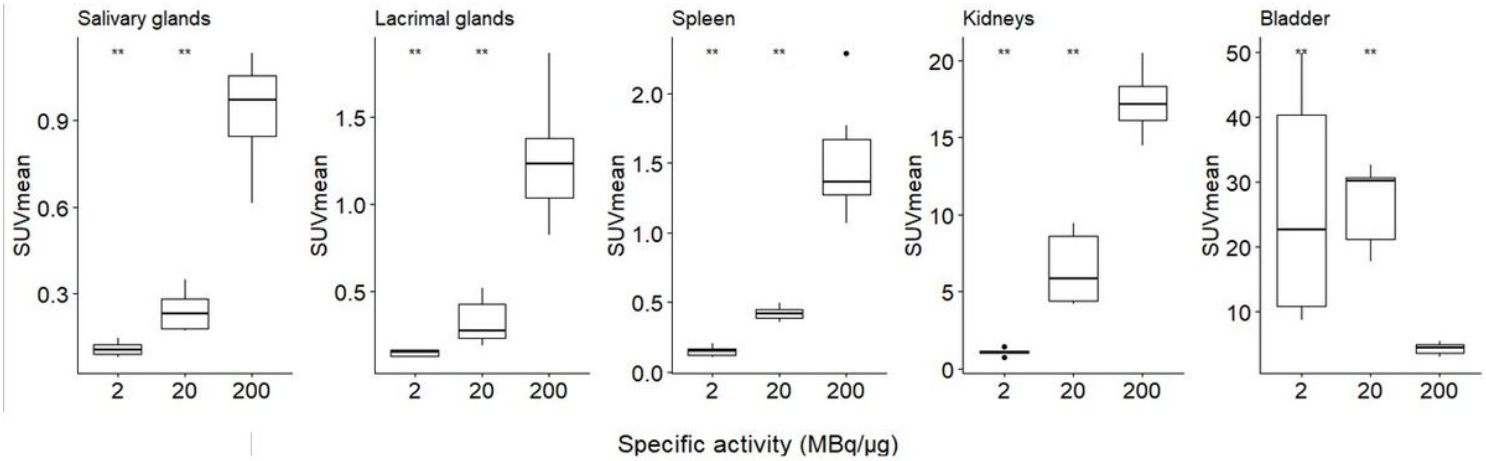

Figure 5

C4-2 xenograft bearing mice were injected with 18F-AlF-PSMA-11 with either a low SA (1.94 ± 0.27 MBq/µg), medium SA (19.10 ± 1.69 MBq/µg) or high SA (196.8 ± 32.4 MBq/µg). Boxplots represent SUVmeanvalues 60 minutes p.i. of PSMA expressing tissues including salivary glands, lacrimal glands, spleen and excretory organs (kidneys and bladder). The high SA was set as reference and the significance level was set at p=0.05. Ns = not significant, ** = p<0.01.

Supplementary Files

This is a list of supplementary files associated with this preprint. Click to download.

- Supplementarydata.docx